

Aharonov-Bohm phase as quantum gate in two-electron charge qubits

A. Weichselbaum and S. E. Ulloa

Department of Physics and Astronomy, Nanoscale and Quantum Phenomena Institute, Ohio University, Athens, Ohio 45701

(Date: Mar 02, 2004)

We analyze the singlet-triplet splitting on a planar array of quantum dots coupled capacitively to a set of external voltage gates. The system is modelled using an extended Hubbard Hamiltonian keeping two excess electrons on the array. The voltage dependence of the low-energy singlet and triplet states is analyzed using the Feshbach formalism. The formation of a well decoupled two-level system in the ground state is shown to rely on the fact of having two particles in the system. Coherent operation of the array is studied with respect to single quantum bit operations. One quantum gate is implemented via voltage controls, while for the necessary second quantum gate, a uniform external magnetic field is introduced. The Aharonov-Bohm phases on the closed loop tunnel connections in the array are used to effectively suppress the tunneling, despite a constant tunneling amplitude in the structure. This allows one to completely stall the qubit in any arbitrary quantum superposition, providing full control of this interesting quantum system.

PACS numbers: 03.67.Lx, 03.65.Vf, 85.35.Be, 85.35.Gv

I. INTRODUCTION

Semiconductor quantum dot systems have been studied extensively in recent years. These quantum dots (qudotes) typically contain from a few to a few hundreds of extra-electrons and are externally controlled by voltage gates. Their behavior at low bias voltages can be well understood by looking at the energetically topmost electrons in the qudot.¹ For an even number of electrons, they may pair up such that the total spin is zero and the topmost two electrons essentially form a singlet, a system that has been proposed as a possible source for entangled electrons.² However, under special circumstances, the ground state may actually be a triplet even without the presence of an external magnetic field.³ A straightforward explanation for this behavior can be given in terms of the exchange contribution to the energy from the two topmost electrons for the case of nearly degenerate single particle levels.¹ For an odd total number of electrons on a single qudot, the overall spin is typically found to be $1/2$.

In this paper we consider an ensemble of qudots, specifically a 2×2 array of interconnected and interacting qudots similar to the typical cellular automata unit cell format.^{4,5,6,7,8} The interaction is modelled within a capacitance matrix formalism. In the weak tunneling regime, the direct exchange energy from the two-body interaction between electrons on different qudots is negligible. Residence of these two electrons on the same qudot (double occupancy) is energetically unfavorable due to the comparatively large Coulomb charging energies. The 2×2 array is considered as a particular implementation of a charge quantum bit (charge qubit). As shown in [9], it is essential for the single qubit operations of such a charge qubit to have a non-local potential, tuneable tunneling amplitudes or an external magnetic field which provides a complex phase to the wavefunction. Since the direct exchange contribution with charges on different dots is negligible, there are no non-local potential effects here.

Further, the tunneling amplitude is considered constant, fixed by the specific realization of the solid state qudot array which typically uses oxide barriers between qudots, and are then basically unaltered by potential gates. In this context of a fixed geometry, the only way to implement full single qubit operations is using an external magnetic field which can be controlled at will.⁹ It is further considered that the field is uniform within the area of the qudot array as is likely the case in normal implementations.

Due to the geometrical symmetry of the qudot array, the ground state turns out to be exactly degenerate for the triplet states when no magnetic field and no gate voltages are applied. However, the spectrum exhibits a gap for the singlet states which is related to the distinct symmetry under particle exchange for the singlet and triplet states. Therefore, particle exchange does play an essential role, yet it is a higher order effect, similar to superexchange¹⁰, as the exchange of two particles on the qudot array takes more than one tunneling step and explores virtual higher energy states.

The properties of the singlet and triplet states are determined by two remaining parameters, the asymmetrically applied gate voltage V_g , which breaks the 90 degree symmetry, and the external magnetic field B perpendicular to the array. We show that careful control of the magnetic flux through the system allows one to rotate the qubit Bloch vector about an axis orthogonal to the one provided by V_g . These two parameters then, provide full quantum manipulation of the charge qubits.

The analysis of our numerical results follows the Feshbach formalism (App. A) which provides an effective Hamiltonian of the two relevant dimensions of the qubit subspace, well decoupled energetically from higher lying states. This approach provides insights on the nature of the system dependence on fields, and explains the ability of the magnetic field to complete the set of necessary single qubit operations.

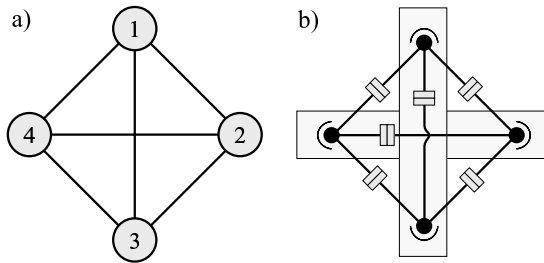


FIG. 1: Setup of 2×2 array. (a) Arrangement of the four islands with mutual tunnel connection indicated by black lines. (b) Same as in (a) but shows explicitly tunneling junctions and capacitive coupling including the two voltage gates acting along the square diagonals.

II. THE MODEL SYSTEM

We examined a range of different geometries of planar arrays with capacitively coupled quantum dots. The best decoupled quantum 2 level systems (qu2LS) in the ground state were found to exhibit high spatial symmetry, i.e. C_{4v} symmetry, in agreement with the requirement of spatially distinct wave functions needed to participate in the qu2LS.⁹ The C_{4v} symmetry of the 2×2 array, for example, ensures a binary groundstate system that for weak inter-dot tunneling is well decoupled energetically from the remainder of the spectrum. Other geometries are clearly possible, but we have chosen here one of the simplest closed loops with C_{4v} symmetry to demonstrate the main concepts.

The model network under consideration is a 2×2 array of qudotes with a single spatial state per site plus spin. The system is sketched in Fig. 1a. As explicitly outlined in panel (b), tunneling is allowed between any pair of dots, where every tunnel junction also carries capacitance. The parameters which enter the model are: the dot-gate capacitance ($C_g = 25\text{aF}$), the dot-dot capacitances ($C_{dd} = 25\text{aF}$ for nearest neighbor dots and 17aF for dots connected through the diagonal of the array), the dot self-capacitance ($C_{d0} = 25\text{aF}$) and the dot-dot tunneling amplitude ($t = 2\mu\text{eV}$). The parameters have been chosen such that the energy cost for double occupancy of a dot (standard Hubbard U) is about 1meV , a commonly used value for these systems, and corresponding to typical dot dimensions of 100nm . Further, the tunneling t must not be chosen too large since otherwise the quality of the 2-level system in the groundstate as well as the well-defined charge per dot are compromised, as we will see below.

The Hamiltonian used to describe this system is of the extended Hubbard type

$$H = \sum_{i,\sigma} \varepsilon_{i\sigma} c_{i\sigma}^\dagger c_{i\sigma} - \sum_{i,j,\sigma} t_{ij}^\sigma (c_{i\sigma}^\dagger c_{j\sigma} + c_{j\sigma}^\dagger c_{i\sigma}) + \frac{1}{2} \sum_{i,j,\sigma,\sigma'} V_{ij} c_{i\sigma}^\dagger c_{j\sigma'}^\dagger c_{j\sigma'} c_{i\sigma} + \sum_i V_i \hat{n}_i \quad (1)$$

with $\hat{n}_i \equiv c_{i\uparrow}^\dagger c_{i\uparrow} + c_{i\downarrow}^\dagger c_{i\downarrow}$ and $c_{i\sigma}^\dagger$ the typical creation operator for a particle at qudot i with spin σ . $\varepsilon_{(i)\sigma}$ refers to the local energy of state σ on the $i = \{1, \dots, n\}$ identical dots and can be used to account for the Zeeman splitting of spins in an external magnetic field. Throughout this paper, however, the ε_σ are simply set equal and zero. The tunneling coefficients t_{ij}^σ from dot i to dot j are considered independent of the spin orientation, thus $t_{ij}^\uparrow = t_{ij}^\downarrow \equiv t_{ij}$. Furthermore, the tunnel connections are considered to be the same up to a phase, i.e. $|t_{ij}| \equiv |t|$. The electrostatic energy in the last two terms of Eq. (1), i.e. the coefficients V_{ij} and V_i , are derived from the total capacitance matrix of the system which is approximated by the capacitor network indicated in Fig. 1b.⁹

An essential property of singlet and triplet states is the effective separation of the spin degree of freedom from the spatial wavefunction component since the total state is a product of spatial and spin components. Here the (anti)symmetry of the spatial wavefunction of (triplet) singlet states under particle exchange is taken care of by imposing (anti)commutator relations on the creation and annihilation operators c_i^\dagger and c_i with the spin index dropped, yet keeping the constraint of a total of two electrons.

An external magnetic field perpendicular to the network of qudotes affects the system insofar as spatial propagation is associated with the acquisition of a complex phase. Therefore the t_{ij} become complex¹¹

$$t_{ij} = t_{ji}^* = |t_{ij}| e^{i\varphi_{ij}}, \quad \text{with } \varphi_{ij} \equiv \frac{e}{\hbar} \int_{x_i}^{x_j} \vec{A} \cdot d\vec{l}, \quad (2)$$

where \vec{A} is the vector potential of the applied magnetic field, $\vec{B} = \vec{\nabla} \times \vec{A}$. Using a symmetric gauge, the acquisition of phase in the 2×2 array of qudotes is indicated in Fig. 2a. The phase *flows* clockwise on the outer connections while the diagonal connections remain phaseless. The ring structure leads to an Aharonov-Bohm phase (AB) for a single particle moving around the ring. Note, however, that the second particle is essential for the necessary ground state qu2LS needed in the qubit setup. For lithographic setups on the scale of 200nm , the required magnetic field for an AB phase cycle on the whole array is around 100mT and thus rather small. At these fields the local wave functions in the individual quantum dots do not change much, and the absolute value of the tunneling $|t|$ is considered constant.

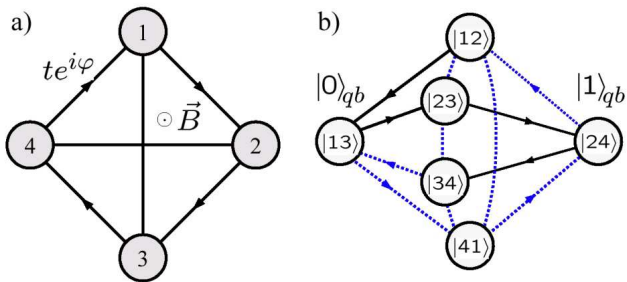


FIG. 2: 2×2 qudot array. (a) Array with a perpendicular magnetic field applied. (b) Schematic network of the Hilbert space states with tunneling transitions between them indicated by connecting lines (states of double occupancy are not included). The arrows indicate the flow of complex phase acquired from a magnetic field in the tunnelling coefficients $|t|e^{i\varphi}$. The dashed blue lines indicate paths of particle exchange (see text). $|0\rangle_{qb} \equiv |13\rangle$ and $|1\rangle_{qb} \equiv |24\rangle$ indicate the qubit states where $|ij\rangle$ are the two electron states with one electron on dot i and the other on dot j .

In Fig. 2b, the two-particle Hilbert space and the allowed tunnel transitions are shown for the 2×2 system, for simplicity ignoring states of double occupancy. The blue dashed lines in Fig. 2b are related to particle exchange in the sense that the off-diagonal element in the corresponding triplet Hamiltonian has an extra minus sign due to its fermionic character, as it can also be seen directly from the basis chosen. For example, the transition $|12\rangle$ to $|23\rangle$ can be thought of as the two-step process of one hopping and one exchange, $|12\rangle \rightarrow |32\rangle \rightarrow -|23\rangle$. Any path with an odd number of dashed segments in the Hilbert space of Fig. 2b has an extra minus sign associated with it. Notice also, that if the path in the Hilbert space network of Fig. 2b is closed, then an odd number of dashed segments refers to an effective exchange of the two electrons. More on this later.

III. ANALYSIS

Using the Hamiltonian in Eq. (1), the eigenspectrum for the 2×2 array is shown in Fig. 3a as function of an asymmetric gate voltage drag V_g , with no magnetic field applied ($B = 0$). For small V_g , the singlet (triplet) low-energy level set of interest is well separated from the remaining singlet (triplet) spectrum. In contrast to the singlet set, however, which has an anticrossing at $V_g = 0$, the triplet set is degenerate there. Panel (b) shows the eigenspectrum as function of the magnetic field when there are no gate voltages applied ($V_g = 0$). The tunneling has been chosen relatively large ($|t| = 5\mu\text{eV}$) such that the energy splitting δ due to the tunneling in the low-energy singlet set (the qu2LS we will focus on) reaches about 1/10 of the distance to the nearest higher lying states, Δ . This is still a good qubit configuration, as the coherent state manipulation in the qu2LS can be per-

formed without significant admixture of the higher lying states. However, the gates must be switched smoothly enough for the evolution to be adiabatic with respect to the higher lying states, as will be seen later from the numerical analysis.

The energy spectrum in Fig. 3b is periodic in the magnetic field in the usual AB sense. Since φ relates to one quarter of the phase on the entire outer loop, this means that with every $\Delta\varphi = 2\pi/4$ one additional flux quantum enters or leaves the cross-sectional area of the array. This is seen for example in the splitting of the singlet which opens and closes with a period $\Delta\varphi = 2\pi/4$. The exact period of the system, however, is $\Delta\varphi = \pi$. Note, that this is not because of the usual $t \rightarrow -t$ symmetry which does not hold here because of the diagonal cross link in the array shown in Fig. 2a. Instead, it can be related to changing the sign in both basis states of the qu2LS. This is easily seen for $\varphi = \pi$ from Fig. 2b by considering $|0\rangle_{qb} \equiv |13\rangle = -|31\rangle$ and dropping all the arrows shown.

Now the essential effect of the magnetic field is that it allows one to close the gap in the singlet qu2LS while at the same time it opens a gap in the triplet qu2LS (at fixed S_z). The smallest magnetic field where this happens is at $\varphi \equiv \varphi_0 = 0.286\pi$, indicated by the arrow in Fig. 3b. The important consequence of tuning the magnetic field to $\varphi \rightarrow \varphi_0$ is that the charge qubit can be held *frozen* in its state by also having $V_g = 0$ (see below).

Figure 3c and d show the singlet ground state configuration and its two *spatially distinct* basis states, respectively. Note that in order to have (close to) degenerate groundstate qu2LS, there must exist a basis representation that is spatially complementary⁹, in agreement with what is shown in panel (d).

In the context of quantum computation, any linear superposition of the two states forming the qubit must be possible.¹² The problem is conveniently mapped into a pseudo spin Hamiltonian with its equivalent 2-level system. The general qubit state $|\psi\rangle = (c_1, c_2)$ when written as a density matrix $\rho = |\psi\rangle\langle\psi| \equiv \frac{1}{2}(1 + \vec{r}_b \cdot \vec{\sigma})$ defines the 3D Bloch vector \vec{r}_b which then is used as the representation of the qubit state.¹² Within this frame, an arbitrary qubit operation translates into a rotation of the Bloch vector (pseudo spin) anywhere in its 3D domain. Two distinct rotations are sufficient to do so. The rotations in pseudo spin language are then generated by the Pauli matrices $\sigma_{\{x,y,z\}}$ and the requirement of two distinct rotations translates into two distinct quantum gates (qugates) that can be built from the Pauli matrices.

For the charge qubit encoded in the 2×2 array with the basis states as shown in Fig. 3d, the physical quantum gates are now as follows: the asymmetrically applied gate voltage (see Fig. 1b) only drags apart the potentials of the two qubit basis states in Fig. 3d and thus represents the σ_z -gate, also referred to as V -gate. On the other hand, the singlet gap or anticrossing can be related to a real off-diagonal element in the 2D pseudospin Hamiltonian which can be tuned down to exactly zero by a magnetic field as shown above. Thus this is referred

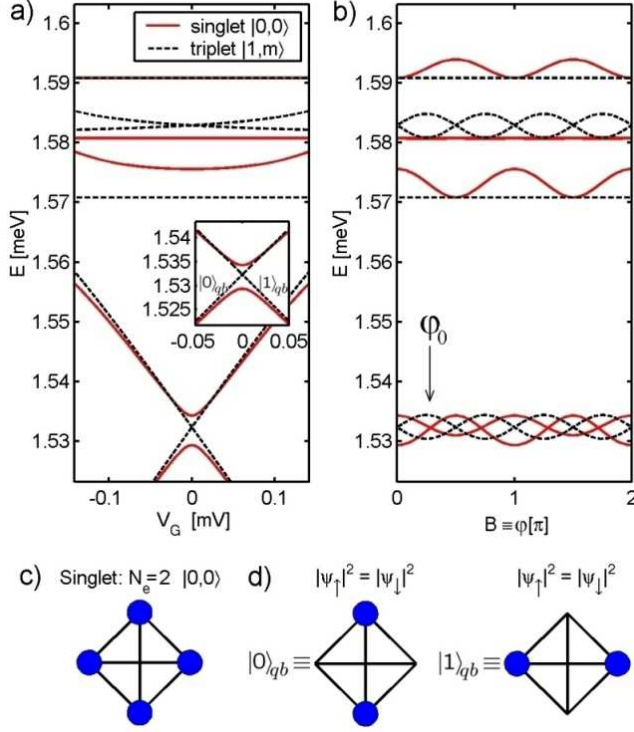


FIG. 3: Energy spectra for the qu2LS of the 2×2 qudot system together with a few higher lying states for singlet and triplet states ($|S, S_z\rangle = |0, 0\rangle$ and $|S, S_z\rangle = |1, m = -1, 0, 1\rangle$ respectively). (a) Energy spectrum vs. asymmetrically applied gate voltage, $V_G \equiv V_{g1} = -V_{g2}$. The doubly occupied states lie about 1meV higher in energy (outside figure) and therefore have negligible influence. The inset shows a closeup of the (anti)crossing in the qu2LS. (b) Energy spectrum vs. uniform external magnetic field perpendicular to the array expressed through the phase in $t = |t| e^{i\varphi}$. The initial singlet anticrossing at $\varphi = 0$ is completely closed for $\varphi = \varphi_0 = 0.286 \pi$, indicated by the arrow in panel (b), while at the same time the triplet levels show a pronounced anticrossing. (c) Singlet ground state probability distribution over the 2×2 array. This state is a symmetric combination of the basis states shown in panel (d): Probability distribution of the basis states of the singlet qu2LS labelled $|0\rangle_{qb}$ and $|1\rangle_{qb}$ with equal probability to find spin up or spin down, $|\psi_\uparrow|^2 = |\psi_\downarrow|^2$.

to as the σ_x -gate or B -gate. Together, the two physical qugates introduced can be utilized to generate arbitrary rotations of the Bloch vector and thus to construct arbitrary qugates for the qu2LS. Also, since both of the qugates can be turned off completely by setting $V_g = 0$ and turning on a specified magnetic field, this allows to freeze the qu2LS in any arbitrary state at any time.

A. Splitting due to exchange energy

We want to analyze now the reasons for the closing and opening of the gap in the qu2LS, as a way to provide

us with insights into the nature of these states. The Hamiltonian in Eq. (1) is written out explicitly as a six-dimensional matrix in Eq. (3) for two electrons on the 2×2 array where, for simplicity, states of double occupancy are neglected.

$$H = \begin{pmatrix} & |13\rangle & |24\rangle & |12\rangle & |23\rangle & |34\rangle & |41\rangle \\ |13\rangle & \varepsilon_1 & 0 & -t^* & -t & \pm t^* & -t \\ |24\rangle & & \varepsilon_1 & \pm t & -t^* & -t & \pm t^* \\ \hline |12\rangle & & & \varepsilon_2 & \pm |t| & 0 & \pm t \\ |23\rangle & & & & \varepsilon_2 & \pm |t| & 0 \\ |34\rangle & & & & & \varepsilon_2 & \pm |t| \\ |41\rangle & c.c. & & & & & \varepsilon_2 \end{pmatrix} \quad (3)$$

The sign in $-(+)t$ refers to the singlet (triplet) spatial Hamiltonian, respectively, with the complex tunneling t as in Eq. (2). The top row and the left-most column of Eq. (3) indicate the two-particle basis states chosen as shown in Fig. 2b. With $t = 0$, the qu2LS grouped in the upper left 2×2 block of the H matrix is degenerate and all intermediate states are split off by the same energy $\Delta_0 \equiv \varepsilon_2 - \varepsilon_1$ due to symmetry. Here, ε_1 and ε_2 are the overall diagonal contributions arising from the Coulomb interaction at $V_g = 0$.

The Hamiltonian in Eq. (3) can be diagonalized analytically. However, a perturbative approach provides explicit insights on the reasons for the splitting due to exchange of otherwise degenerate states. Furthermore, the setup proves sufficiently simple to allow the complex sum to all orders over all possible histories in Hilbert space within the Feshbach formalism. The result consistently agrees with the analytical solution to the problem.

In order to obtain an estimate for the splitting in the ground state set, the Feshbach formalism provides an effective Hamiltonian for the qu2LS (\mathcal{P} space) coupled to higher lying states (\mathcal{Q} space, see App. A). For convenience, the qu2LS basis is written as $\mathcal{P} \equiv \{|13\rangle, |24\rangle\} \equiv \{|0\rangle_{qb}, |1\rangle_{qb}\} \equiv \{|0, 1\rangle_{qb}$. The remaining intermediate states in Fig. 2b (\mathcal{Q} space) form a ring topology where every node is linked to the $|0\rangle_{qb}$ and $|1\rangle_{qb}$ states. Note that there is no direct transition from $|0\rangle_{qb}$ to $|1\rangle_{qb}$, but one has to proceed through at least one of the intermediate states with an energy cost of $\Delta_0 \equiv \varepsilon_2 - \varepsilon_1$.

The effective $2D$ Hamiltonian for the qu2LS in the absence of a magnetic field is now constructed as follows: the matrix element $(H_{eff})_{ij}$ with $i, j = \{0, 1\}_{qb}$ is the sum over all possible paths that start in state i , immediately proceed to intermediate states \mathcal{Q} , and only in the final step come back to state j . The number of possible paths constructed in this manner for a total of n steps is $S_n(i, j) \equiv 2^n$ with $n \geq 2$ since there are 4 possibilities to go from $|i\rangle$ to the intermediate states, then 2 possibilities of which way to go in the ring at each of the $n - 2$ intermediate steps, and 1 choice left to finally leave the ring and go to state $|j\rangle$. Furthermore, for $n > 2$, exactly half of these paths include particle exchange, i.e. have an odd number of dashed lines in Fig. 2b, and thus for

the case of the triplet states cancel each other to zero. The underlying reason for this is the spatial C_{4v} symmetry of the 2×2 setup which has two mirror symmetry planes perpendicular to the array. Therefore, for every path starting from $\{0, 1\}_{qb}$ and ending in $\{1, 0\}_{qb}$ has a mirrored counterpart where the particles are exchanged in the final state as compared to the first path.

The case $n = 2$ needs separate consideration. For the diagonal elements in H_{eff} the same step is taken twice, back and forth, and thus the relative sign in t does not matter. Therefore the triplet states have an $n = 2$ contribution in the diagonal. Putting all these pieces together, yields the matrix elements for the effective Hamiltonian which, for example, in case of the singlet states are

$$\begin{aligned} \langle i | H_{eff} | j \rangle_S &= \varepsilon_1 \delta_{ij} + \frac{(-2t)^2}{\omega - \varepsilon_2} \sum_{m=0}^{\infty} \left(\frac{-2t}{\omega - \varepsilon_2} \right)^m \\ &= \varepsilon_1 \delta_{ij} + \frac{(-2t)^2}{\omega - \varepsilon_2 + 2t} \equiv \varepsilon_1 \delta_{ij} + \Sigma_{ij}^S(\omega), \end{aligned} \quad (4)$$

and thus

$$H_{eff}^{singlet}(\omega) \equiv \begin{pmatrix} \varepsilon_1 & 0 \\ 0 & \varepsilon_1 \end{pmatrix} + \frac{4t^2}{\omega - \varepsilon_2 + 2t} \begin{pmatrix} 1 & 1 \\ 1 & 1 \end{pmatrix} \quad (5a)$$

$$H_{eff}^{triplet}(\omega) \equiv \begin{pmatrix} \varepsilon_1 & 0 \\ 0 & \varepsilon_1 \end{pmatrix} + \frac{4t^2}{\omega - \varepsilon_2} \begin{pmatrix} 1 & 0 \\ 0 & 1 \end{pmatrix}, \quad (5b)$$

where for the triplet state only the paths with $n = 2$ contribute. The eigenstates for the qu2LS are now obtained from the nonlinear eigensystem $H_{eff}(\omega) |\psi\rangle = \omega |\psi\rangle$ where $|\psi\rangle$ is restricted to the $2D$ ground space. $H_{eff}^{triplet}$ is still diagonal, and therefore the triplet states *do not mix* with each other, but are just shifted lower by $\frac{\Delta_0}{2} - \sqrt{\left(\frac{\Delta_0}{2}\right)^2 + 4t^2} = -\frac{4t^2}{\Delta_0} + \mathcal{O}(t^3)$, with $\Delta_0 = \varepsilon_2 - \varepsilon_1$. The singlet states, however, rearrange to symmetric and antisymmetric combinations of the original basis. One of the eigenstates remains at the original eigenenergy $\omega = \varepsilon_1$, while the second one is lowered by δ given as

$$\delta \equiv \left(\frac{\Delta_0}{2} - t \right) - \sqrt{\left(\frac{\Delta_0}{2} - t \right)^2 + 8t^2} = -\frac{8t^2}{\Delta_0} + \mathcal{O}(t^3) \quad (6)$$

and thus forms the ground state of the system for finite t . The analytical solutions are consistent with the numerical diagonalization of the Hamiltonian in Eq. (3).

B. Effect of a magnetic field

We apply again the Feshbach formalism to the system in Fig. 2b, but now including the complex phases indicated by the arrows in that figure. Note that the phases due to the magnetic field affect only the first and last step in each path, while intermediate state transitions remain unaltered by the presence of the magnetic field

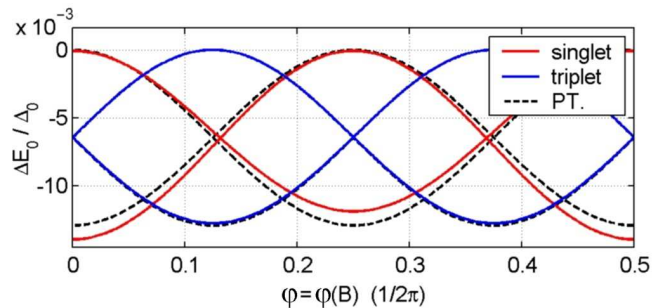


FIG. 4: Energy splitting in the qu2LS for the system of Eq. 3 in dependence of the magnetic field for singlet (red) and triplet states (blue). The splitting is shown in units of $\Delta_0 = \varepsilon_2 - \varepsilon_1$, namely the separation of the qu2LS from the remaining Hilbert space. The dashed black line is the result of the lowest order Feshbach analysis, Eq. (7).

since they correspond to transitions through the diagonal of the array in Fig. 2a (there are no arrows on the transitions between intermediate states in Fig. 2b).

The paths can be summed up similarly. For simplicity, however, we give only the contribution to lowest order in t for the effective Hamiltonian. The denominator $\omega - \varepsilon_2$ is then replaced by $\varepsilon_1 - \varepsilon_2 = -\Delta_0$, and so the lowest order contribution to the self energy term is

$$\Sigma_{eff}^{singlet}(\omega, \varphi) = -\frac{4t^2}{\Delta_0} \begin{pmatrix} 1 & \cos 2\varphi \\ \cos 2\varphi & 1 \end{pmatrix} + \mathcal{O}(t^3) \quad (7a)$$

$$\Sigma_{eff}^{triplet}(\omega, \varphi) = -\frac{4t^2}{\Delta_0} \begin{pmatrix} 1 & i \sin 2\varphi \\ -i \sin 2\varphi & 1 \end{pmatrix} + \mathcal{O}(t^3). \quad (7b)$$

Comparing this with the last terms in Eqs. (5), the effect of the external magnetic field is obvious. With increasing φ the singlet splitting can be reduced down to zero, while simultaneously a comparable gap opens in the triplet states, in agreement with the numerical data for the full 2×2 system in Fig. 3b. The effect of the magnetic field on the singlet (triplet) states is that of a σ_x (σ_y) gate, and thus clearly provides the necessary second quantum gate for single qubit operation. Figure 4 compares the exact numerical results of the Hamiltonian in Eq. (3) with above lowest order perturbative approach for the splitting in the qu2LS. The lowest order contribution in the Feshbach formalism already provides an excellent approximation.

C. Numerical qubit dynamic

The time evolution of the 2×2 qudot array is studied numerically for the singlet state under the action of the V -gate (σ_z) and the B -gate (σ_x). Note that here the B -gate is considered non-active when a magnetic field is tuned to the phase $\varphi = \varphi_0$ indicated by the arrow in Fig. 3b, while the gate is considered active when the magnetic field is turned off ($\varphi = 0$). In this sense, with

none of the two gates applied, the system is *static* since the singlet states are degenerate. Typical time dynamics data is shown in Fig. 5. Starting in the singlet ground state (Bloch vector $\vec{r}_b = +\hat{x}$), the system is static at $t = 0$. The following V -gate rotates this state around the \hat{z} axis by 450° , ending in $\vec{r}_b = +\hat{y}$, where the system is stalled for a short time interval until the B -gate is activated at $t = 1.6\text{ns}$. Now the B -gate rotates \vec{r}_b around the \hat{x} -axis again by 450° , leaving the state in the $+\hat{z}$ state where the system is stalled again at $t = 3\text{ns}$, now being in the central region on the time axis in figure Fig. 5b. Since $\pm\hat{z}$ corresponds to the basis states of the qubit, the charge distribution equals the $|1\rangle_{qb}$ state in Fig. 3d as can be seen by the snapshots shown along the time evolution in between panels (a) and (b) in Fig. 5. After another B -gate of the same duration, the system is rotated another 450° around the \hat{x} -axis leaving the qubit in the $-\hat{y}$ state at $t = 4.8\text{ns}$. When finally a $(-V)$ -gate is applied, the qubit is rotated by -450° around the \hat{z} -axis and the system is left in the $-\hat{x}$ configuration at $t = 6.2\text{ns}$. The time evolution of the Bloch vector in this whole process sweeps two grand circles in the Bloch sphere, as shown in the inset of panel (b).

The numerical data shown in Fig. 5 confirms the previous analysis. The main point is that the qubit can be placed into any state by applying appropriate magnetic field and gate voltages to the system, yielding full control of the qubit as desired.

IV. CONCLUSIONS

Singlet and triplet states have been studied on a planar array of quantum dots. With respect to qubits, a two-fold nearly degenerate ground state pair was constructed and the splitting of this two-level system was explained and estimated using the Feshbach formalism. Furthermore these states were shown to represent full single qubit operations encoded in the charge states. The AB flux given by a uniform magnetic field provides the required second quantum gate by generating a dynamical phase in the wave function of the two electron qubit state. This can be used to effectively turn off the qubit dynamics at will.

Acknowledgments

We acknowledge helpful discussions with A. Govorov and with D. Phillips (especially for suggesting to us the Feshbach formalism), as well as support from NSF Grant NIRT 0103034, and the Condensed Matter and Surface Sciences Program at Ohio University.

APPENDIX A: FESHBACH FORMALISM

The Feshbach formalism provides an efficient procedure to reduce the full Hamiltonian of a large (possibly

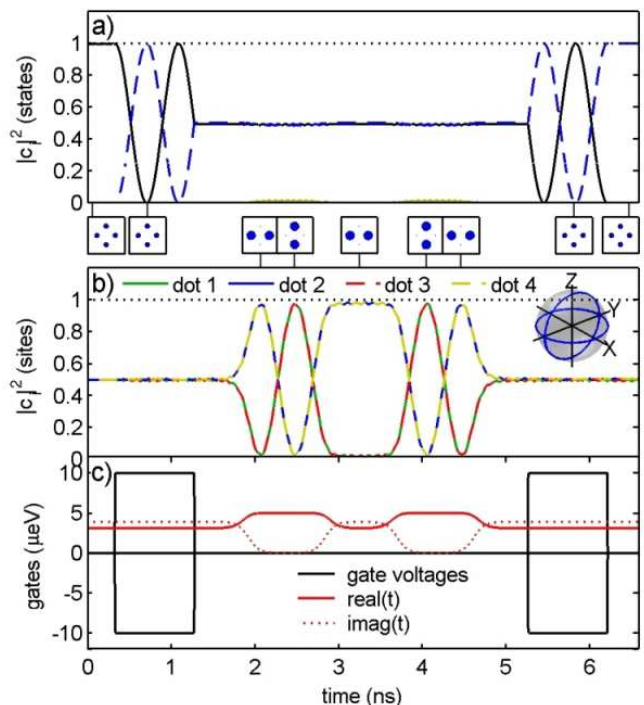


FIG. 5: Time evolution and control of the singlet qu2LS on the 2×2 array. (a) Time evolution of the state occupancy with respect to the qubit basis $|0\rangle_{qb}$ and $|1\rangle_{qb}$ (see Fig. 3d). (b) Time evolution of the site occupancy $|\langle c_i^+ c_i \rangle|^2 \equiv |\langle \psi | c_i^+ c_i | \psi \rangle|^2$. The square panels in between panels (a) and (b) show snapshots of the charge distribution on the array at the times indicated either towards panel (a) or panel (b). The inset in panel (b) shows the time evolution of the qubit in Bloch sphere representation. (c) Time dependence of the voltage gates (black) and the magnetic field expressed through $\text{Re}(t)$ and $\text{Im}(t)$ (red lines) where $\text{Abs}(t)$ is kept constant. The time constant for rise and fall time of the gate voltages was chosen as $\tau_V \equiv 0.658$ ps while for the tunneling the considerably longer $\tau_\varphi \equiv 100 \cdot \tau_V = 65.8$ ps was used out of adiabatic purposes with respect to the higher lying states.

infinite) system to the Hamiltonian of a small (finite) subsystem which should be energetically well separated from the remainder of the space.¹³ Given a finite subspace \mathcal{P} of the total Hilbert space \mathcal{H} with its complement \mathcal{Q} , such that $\mathcal{P} + \mathcal{Q} = \mathcal{H}$, the projections into these spaces are $P \equiv \sum_{i \in \mathcal{P}} |i\rangle \langle i|$ and $Q \equiv \sum_{k \notin \mathcal{P}} |k\rangle \langle k| = 1 - P$, respectively. The stationary Schrödinger equation when projected into the \mathcal{P} and \mathcal{Q} spaces becomes

$$\begin{pmatrix} H_{PP} & H_{PQ} \\ H_{QP} & H_{QQ} \end{pmatrix} \begin{pmatrix} |\psi_P\rangle \\ |\psi_Q\rangle \end{pmatrix} = E \begin{pmatrix} |\psi_P\rangle \\ |\psi_Q\rangle \end{pmatrix} \quad (\text{A1})$$

with the projections defined as $H_{PQ} \equiv PHQ$, $|\psi_P\rangle \equiv P|\psi\rangle$, and similarly for the remaining ones. By assumption, \mathcal{P} has finite dimension, thus H_{PP} is also finite. $|\psi_Q\rangle$ can be formally eliminated from Eq. (A1) and the result

is $H_{eff}^P |\psi_P\rangle = E |\psi_P\rangle$ with

$$H_{eff}^P \equiv H_{PP} + \underbrace{H_{PQ} \frac{1}{E - H_{QQ}} H_{QP}}_{\equiv \Sigma_{QQ}(E)}, \quad (\text{A2})$$

with H_{eff}^P describing the effective Hamiltonian in space \mathcal{P} . H_{eff}^P is thus the sum of the unperturbed matrix elements H_{PP} and the *self-energy* contribution Σ_{QQ} . Note that Eq. (A2) is still exact and thus must be nonlinear in E in order to represent the entire eigenspectrum of the system. The non-linearity is manifested in the E dependence of Σ_{QQ} . It ensures a good approximation while it does not result in further complications here, since for the two-dimensional space \mathcal{P} discussed in this paper, the resulting equations can be conveniently solved analytically.

If the full Hamiltonian H did not couple the \mathcal{P} and \mathcal{Q} spaces, then with $H_{PQ} = 0$ the second term Σ_{QQ} in Eq. (A2) vanishes consistently. Note also that eliminating $|\psi_Q\rangle$ from Eq. (A1) eliminates the coefficients of $|\psi_Q\rangle$

so that this procedure systematically eliminates variables on the large scale. Eq. (A2) is a formal solution since the self-energy $\Sigma_{QQ}(E)$ is not known. But there are different ways to approximate Σ_{QQ} using perturbative expansions naturally suggested by its definition. With the identity

$$\frac{1}{\omega - (H_0 + V)_{QQ}} = \frac{1}{\omega - H_{0,QQ}} \sum_{n=0}^{\infty} \left(V_{QQ} \frac{1}{\omega - H_{0,QQ}} \right)^n, \quad (\text{A3})$$

a very useful generalization of the Brillouin-Wigner formalism to more than one, but still a finite number of states, is obtained.¹⁴ This approach is essentially a path formulation in Hilbert space in the sense that *all possible path histories through Hilbert space* are taken, starting in \mathcal{P} , proceeding directly into \mathcal{Q} (H_{PQ} in Eq. A2) and only in the final step returning back to \mathcal{P} (H_{QP} in Eq. A2). In addition, every intermediate step is weighted by the *propagator* terms $\langle k | (E - H_{QQ}^0)^{-1} | k \rangle = (E - \varepsilon_k)^{-1}$ (Eq. A3). The lowest order contributions are then equivalent to the shortest histories through \mathcal{Q} space with lowest cost in energy.

¹ S. Tarucha, D. Austing, Y. Tokura, W. van der Wiel, L. Kouwenhoven, Phys. Rev. Lett. **84**, 2485 (2000).

² D. Saraga and D. Loss, Phys. Rev. Lett. **90**, 166803 (2003).

³ A. Fuhrer, T. Ihn, K. Ensslin, W. Wegscheider, M. Bichler, Phys. Rev. Lett. **91**, 206802 (2003).

⁴ G. Toth and C. S. Lent, Phys. Rev. A **63**, 052315 (2001).

⁵ I. Amlani, A. Orlov, G. Toth, G. Bernstein, C. Lent, and G. Snider, Science **284**, 289 (1999).

⁶ C. Lent, Science **288**, 1597 (2000).

⁷ M. Lieberman, S. Chellamma, B. Varughese, Y. Wang, C. Lent, G. Bernstein, G. Snider, F. Peiris, Ann. N.Y. Acad. Sci. **960**, 225 (2002).

⁸ F. Rojas, E. Cota, and S.E. Ulloa, to appear in IEEE Transactions on Nanotechnology (2004).

⁹ A. Weichselbaum, S. E. Ulloa, cond-mat/0401106 (2004).

¹⁰ J. Jefferson, W. Häusler, Phys. Rev. B **54**, 4936 (1996).

¹¹ R. Peierls, Z. Phys. **80**, 763 (1933).

¹² M. Nielsen, I. Chuang, (Cambridge University Press, 2000).

¹³ H. Feshbach, *Ann. Phys. (N.Y.)* **19**, 287 (1962).

¹⁴ N. H. March, W. H. Young, S. Sampanthar, (Cambridge University Press, 1967).